



Characterization of the friction parameters of Harmonic Drive actuators

P. Chedmail,^a J.-P. Martineau^{a,b}

^a*Laboratoire d'Automatique de Nantes, Ecole Centrale de Nantes, 1 rue de la Noë, 44072 Nantes Cedex 03, France*

^b*Ecole Navale, Lanvéoc-Poulmic, 29200 Brest naval, France*

ABSTRACT

The control of rigid and flexible robots is performed using models for predicting the behaviour of their structure. It needs to characterize mechanical parameters. We first present the friction phenomenon in the actuators. The usual Coulomb's model of friction combined with viscosity is no more adapted to robot reducers. We have to identify the friction parameters to reduce the control perturbations. We distinguish the static and the quasi-static friction. We verify that the dry friction torque depends on the applied load and on the angular position.

In a second time, we describe the stiffness study. The stiffness of each actuator involves an inaccuracy. It is important to know and correct the angular deflection shift. After a theoretical approach, we will present the experimental results and propose a general model.

1. INTRODUCTION

In order to control a robot, we need to characterise mechanical parameters (Depincé⁹). The transmission introduces some effects — friction, unknown inertia, stiffness, play — which modify the control of the joints. We have to identify them in order to correct the perturbations that they involve. Friction is an important non-linear parameter of the actuators. It reduces both stability and steady state accuracy (Brière^{3&4}, Gaudin-Bessonnet¹², Giovanni & Coll¹³, Gomes-Chretien¹⁵, Chedmail & Coll.¹⁶, Raymond & Coll.¹⁷).

The well known Coulomb's friction model combined with the viscous friction model is classically supposed to be representative of the friction effects in robots actuators — i.e. the motor and the associated reducer — (Gaudin-Bessonnet¹², Giovanni & Coll¹³). A few experiments on flexible robots have encouraged us to pay more attention to the friction modelling (Depincé⁹) because the friction effects may hide other phenomena (inertia and flexibility). More precisely, we intend to describe, in the third paragraph, the global friction effects — these of the motor and the transmission — with respect to the angular output position and the

payload (Chedmail-Martineau⁷).

In the fourth paragraph, we describe the stiffness characterization of an Harmonic Drive actuator, and we propose a model of this type of actuator. The increment velocity, the payload and the friction must be integrated in the model.

2. EXPERIMENTAL DEVICE

The experimental device is an anthropomorphic robot (Chedmail-Martineau⁶). It is composed of three axes and two flexible links (Figure 1). The first link is considered as rigid.

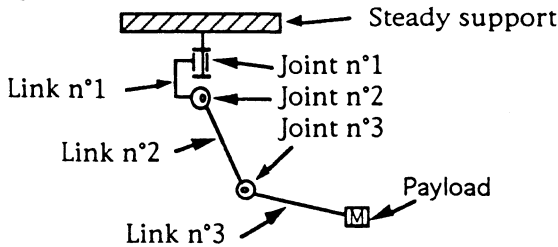


Figure 1 - Scheme of the experimental robot

We consider the joints number 2 and 3 of the robot. Their references are : RKS 32 3030 S and RKS 20 3006 S from Gammatic company (Gammatic¹⁰). They are composed of electrical AC motors and Harmonic Drive reducer. The rated load torque and the admissible peak torque are respectively : 33 mN and 98 mN for joint 2 and 20 mN and 82 mN for joint 3. The reducers are "IH" type. They are supposed to have no play.

As one can see on the Figures 2 and 3, the external torque (Γ_{ext}) is obtained with a given load acting on a pulley. The pulley is fixed on the output shaft. A change of the pay load induces a variation of the external torque.

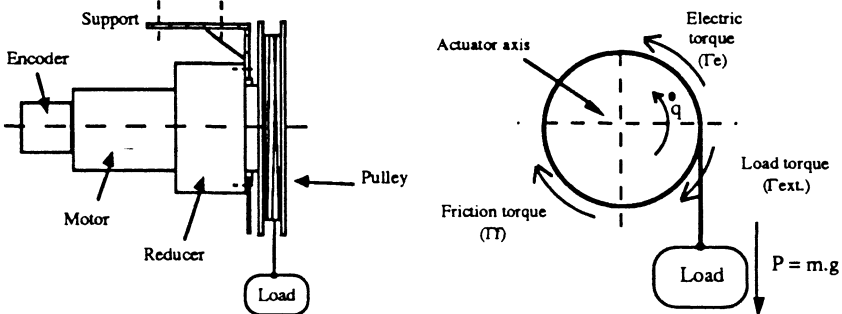


Figure 2 - Scheme of the mechanical aspect / Figure 3 - Principle of the measurement

The encoder accuracy is about 8000 points per turn. The reduction ratio is 100 and the output accuracy is $7.85 \cdot 10^{-6}$ radian. The AC motor is a synchronous type. The nominal velocity of the motor is 3000 tr./min with a 62 W available output power. Motors and reducers are coupled with an Oldham joint. Its nominal angular play is 9" (Gammatic¹⁰).

The control and measurement system is composed of a power cupboard and a

DSPACE computer system developed by Scientific Software (Scientific Software¹⁸). It is integrated on the PC architecture. The main board is composed of a Texas Instrument processor (TMS320C30). It can reach an acquisition frequency of 20 kHz and a computation power of 33,3 Mflops.

3. ANALYSIS OF THE FRICTION TORQUE

3.1. Friction model

The tribology of the Harmonic Drive transmission is very complex because of the flexspline which is due to its particular design. (Figure 4).

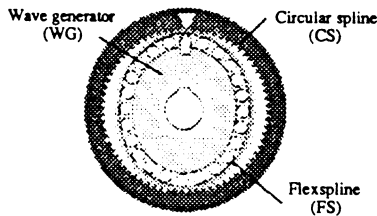


Figure 4 -Principle of the Harmonic Drive reducer

To our knowledge, there are only a few papers which study this subject (Brière⁴, Gogoussis-Donath¹⁴, Raymond & Coll.¹⁷).

In the classical model (Figure 5), there are two kinds of friction effects (Armstrong^{1&2}) : Coulomb's friction (Γ_{fs}), and viscosity (Γ_{fv}). The Coulomb's friction generates a resistant torque during the starting movement. The second friction effect appears when there is a relative movement between the rotor and the stator. There is a zone where measurements are difficult to perform.

In our study, we intend to distinguish the starting friction torque Γ_{fsi} and the equilibrium friction torque (Γ_{fei}) (Figure 5). The first one corresponds to the minimum torque for starting the rotation of the output shaft. The second one is related with the equilibrium torque before stopping. In a usual model, one supposes that $\Gamma_{fs1} = \Gamma_{fe2}$ and $\Gamma_{fs4} = \Gamma_{fe3}$. In our model Γ_{fs1} and Γ_{fe2} (resp. Γ_{fs4} and Γ_{fe3}) are different (Figure 6).

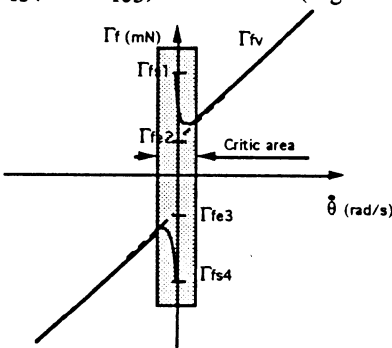


Figure 5 - Stribeck's friction model

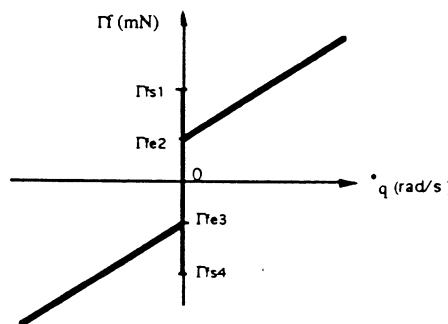


Figure 6 - Selected friction model

3.2. Measurement method

We want to measure, for different loads and positions of the output shaft, the electrical torque (Γ_i) for starting the rotation, or to balance the position after a move of the axis. For each acquisition, we memorize both control voltage U_c and angular position. The experimental proceeding for measuring Γ_2 and Γ_3 , is as follows (Figure 7) :

- 1- Increase the control voltage U_c until detection of a movement.
- 2- Reduce U_c until the rotor stops.
- 3- Memorize the applied voltage $U_c(\Gamma_2)$, and the angular position
- 4- Reduce U_c until the movement is in the opposite sense.
- 5- Increase U_c until the rotor stops.
- 6- Memorize the applied voltage $U_c(\Gamma_3)$ and the angular position.
- 7- Repeat the operation to perform a new measurement.

For the Γ_1 and Γ_4 torques measurement the procedure is as follows (Figure 8) :

- 1- Reach the steady state of the load as in the first proceeding.
- 2- Increase U_c until the starting up of the load.
- 3- Memorize the control voltage $U_c(\Gamma_1)$ and the position of the measurement.
- 4- Reach the steady state of the load
- 5- Decrease the control voltage U_c , until the detection of the downward start of the load.
- 6- Memorize the control voltage $U_c(\Gamma_4)$ and the starting position.
- 7- Repeat the operation to perform a new measurement.

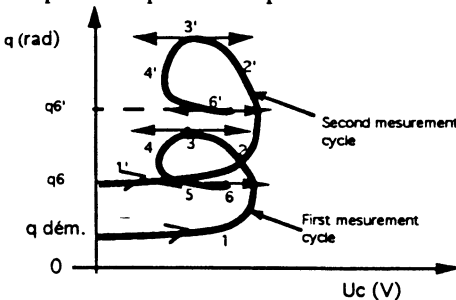


Figure 7 - $U_c(\Gamma_2)$ and $U_c(\Gamma_3)$

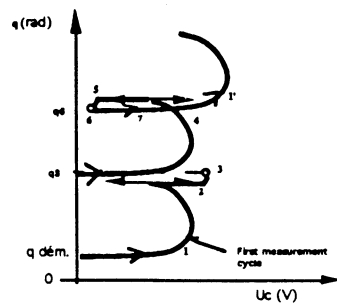


Figure 8 - $U_c(\Gamma_1)$ and $U_c(\Gamma_4)$

The friction torque is always opposed to the movement. Therefore, the quasi-static equilibrium of the actuator is :

$$\Gamma_1 = \Gamma_{ext} + \Gamma_{fs1}, \Gamma_2 = \Gamma_{ext} + \Gamma_{fe2}, \Gamma_3 = \Gamma_{ext} - \Gamma_{fe3}, \Gamma_4 = \Gamma_{ext} - \Gamma_{fs4},$$

where Γ_{ext} is the external load (figure 9).

$$\text{Phase 1-2-3} \rightarrow U_c(\Gamma_2) = U_c(\Gamma_{ext} + \Gamma_{fe2})$$

$$\text{Phase 4-5-6} \rightarrow U_c(\Gamma_3) = U_c(\Gamma_{ext} - \Gamma_{fe3})$$

We don't fix the measurement position. One can see on Figure 10, an example of measurement for $U_c(\Gamma_1)$ and $U_c(\Gamma_2)$ with a 3 Kg load. The mean

value of the starting voltage is about 0.6 V. The mean value of the equilibrium voltage is almost 0.3 V. The two average values are different. Consequently we have to distinguish in the model the starting and equilibrium friction torques.

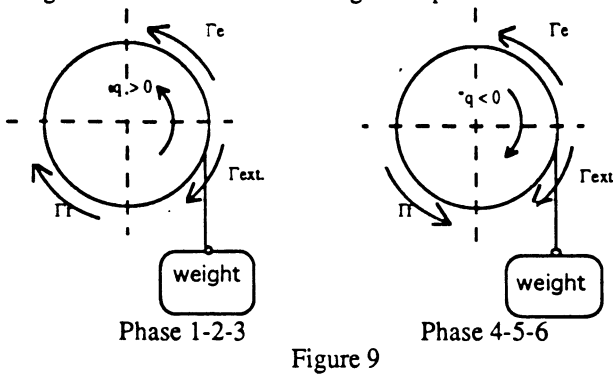


Figure 9

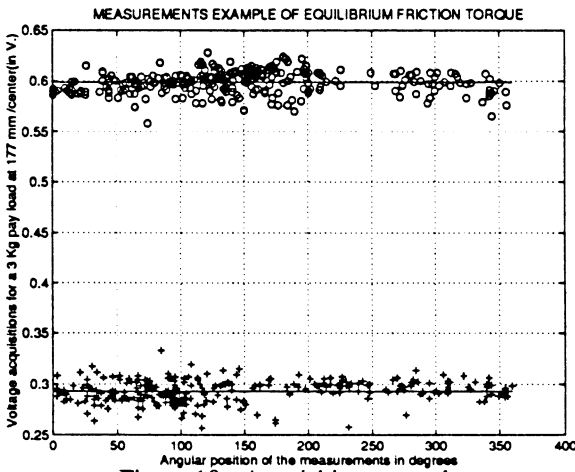


Figure 10 - Acquisition example.

3.3. Results

The curves on Figure 11 represent the electric voltage evolution $U_c(\Gamma_i)$ of the starting and balance situations for different loads (Γ_{ext}) and rotation sense (positive and negative). Each load is tested with at least 100 measurements. Therefore, each point corresponds to their average value. We compute, with a least squares method, the equations of the straight lines (Figure 11 and Figure 12) :

$$U_c(\Gamma_2) = a_2 \Gamma_{ext} + b_2 \quad (1)$$

$$U_c(\Gamma_3) = a_3 \Gamma_{ext} + b_3 \quad (2)$$

We can observe that the friction phenomenon is symmetrical with respect of the load torque sign. In figures 11 to 13, " $U_c(G_i)$ " corresponds to " $U_c(\Gamma_i)$ ".

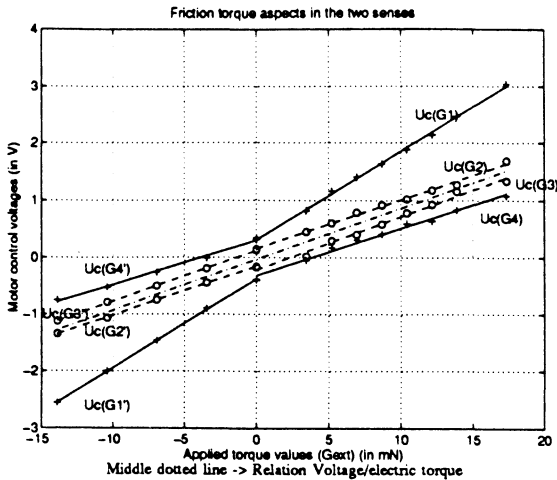
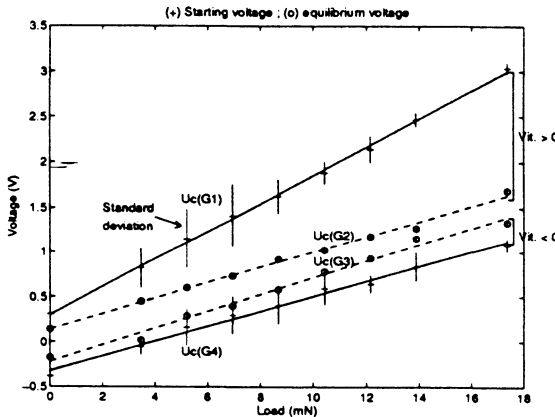


Figure 11


 Figure 12 - Positive torque and standard deviations (electrical image U_c of the electrical torque Γ_i)

Standard deviations are visualized with vertical straight lines which are attached to each average point. The deviations are not the same for each average point ; it is due to the effect of the randomized positions of the starting points of the different measurements (see figure 10) : the friction torque depends on the position of the measurement. The standard deviation is more important for the starting torque (Γ_1 or Γ_4) than for the balance torque (Γ_2 or Γ_3). It means that the starting phenomenon is less foreseeable than the equilibrium one.

Now, let compute the electrical image of the friction torques. We reason with the direct values of the torques.

$$\Gamma_2 (U_c2) = \Gamma_{ext} + \Gamma_{fe2} \quad \text{in the upward motion of the load} \quad (3)$$

$$\Gamma_3(Uc3) = \Gamma_{ext} - \Gamma_{fe3} \quad \text{in the downward motion of the load} \quad (4)$$

The hypothesis of symmetry of the equilibrium friction torque is :

$$\Gamma_{fe2} = \Gamma_{fe3} \quad (5)$$

Combining (1) ... (5), with the hypothesis that $Uc = Uc(\Gamma)$ is linear with respect to Γ we obtain :

$$Uc(\Gamma_{ext}) = \left(\frac{a2 + a3}{2} \right) \Gamma_{ext} + \left(\frac{b2 + b3}{2} \right) \quad \text{and more generally,}$$

$$Uc(\Gamma) = \left(\frac{a2 + a3}{2} \right) \Gamma + \left(\frac{b2 + b3}{2} \right) \quad (6)$$

The identified relation between the input voltage Uc and the electrical torque is :

$$\Gamma = 11.17 Uc + 0.3654 \quad (7)$$

With (6) and the equations $Uc = Uc(\Gamma_i)$ we obtain the linear equations of friction torques : $\Gamma_{fsi} = f_{si}(\Gamma_{ext})$, $\Gamma_{fej} = f_{ej}(\Gamma_{ext})$, $i = 1$ and 4 , $j = 2$ and 3 (figure 13).

Figure 13 proves that the variations of the starting friction torque (Γ_{fsi}) with respect to the external load (Γ_{ext}) can't be neglected. The equilibrium torque (Γ_{fei}) is quasi constant.

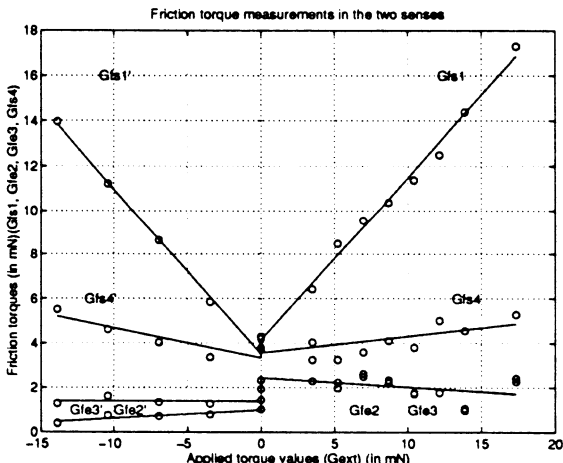


Figure 13

3.4. Influence of the angular position

Our purpose is to evaluate the variation of the friction torque with respect to the angular positions of the drive shaft. We propose two different approaches. A global one evaluates the evolution of the equilibrium torque Γ_{fe} along a turn of the output shaft. A local one analyses — along a fraction of degree — the



variations of Γ_{fe} .

The global approach demonstrates that along a turn, the variation of the friction torque (or its electrical image) is negligible. The standard deviation value is about 3% (0.02 Volt) of the mean value (0.73 Volt) (Figure 14).

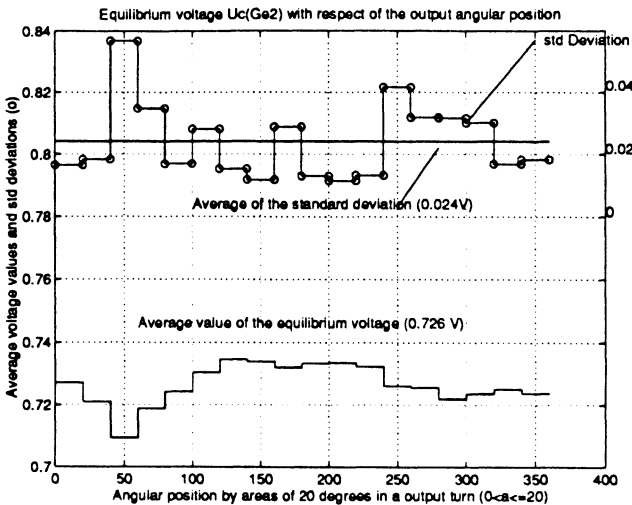


Figure 14

At least, 48 measures are performed in each class of measure (20°).

The local approach has been performed using several methods (Chedmail and Martineau⁷): a spectral analysis, a quasi-static analysis, a statistic analysis.

Each of them leads to the same conclusion: there are two high friction points per turn of the input shaft.

For instance, the spectral analysis is based on a measurement of the velocity with a constant control voltage U_c (and a constant electric torque Γ). The spectrum of the velocity presents a critical frequency. It is a confirmation of the result described in Tuttle²⁰. It corresponds to two high friction points per input turn, i.e., 200 points of high friction per output turn (see Figure 15).

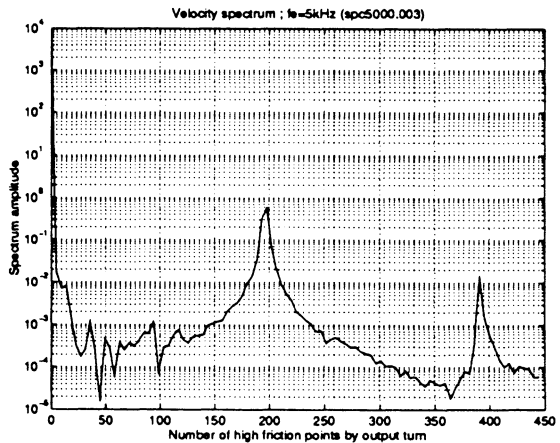


Figure 15

3.5. Conclusion on the friction torque analysis

We have proposed a new modelization of the static friction torques in Harmonic Drive actuators. We have deduced from the experimentations that :

- the starting friction torque Γ_{fs} is proportional to the applied torque,
- the equilibrium friction torque Γ_{fe} weakly depends on the applied torque,
- the starting friction torque can't be neglected in the control law with respect to the applied external torque
- the influence of the angular position is not very important along a turn of the output shaft : the standard deviation is lower than 3% of the mean value of Γ_{fe} . However, we have demonstrated the existence of hard points which frequency is equal to 2 per turn of the input shaft. In our opinion it is due to the existence of a local default of the gears or of the mechanical components.

4. ANALYSIS OF THE REDUCER STIFFNESS

4.1. Stiffness specifications

When one transmits a driving force, there is an elastic deformation in the reducer. If it is a driving torque, this deformation is an angular displacement between the input and the output shaft. Generally the relation is supposed to be linear. This is not the case for the Harmonic drive reducer. Thereafter, we recall the Gammatic model (Gammatic¹⁰) and we compare it to our own results.

4.1.1. Gammatic model of the Harmonic Drive

In a Harmonic Drive reducer, there is a flexible component : "the flexspline" (figure 4). 30% of its teeth are in contact with the circular spline. When the external torque (Γ_{ext}) increases, the flexspline deformation and the surface of contact increase. The stiffness increases simultaneously. Gammatic approximates the stiffness of RKS actuators by a piecewise linear law. The hysteresis losses, which are caused by friction torques, are ignored.

For each reducer, the model has three different stiffness coefficients (Figure 16). The HDUC-IH 20 reducer has the following specifications :

$T1 = 7,8 \text{ mN}$
 $T2 = 25 \text{ mN}$
 $T \text{ max. exceptional } (147 \text{ mN})$
 $K1 = 1,5 \cdot 10^4 \text{ mN/rd}$
 $K2 = 2,6 \cdot 10^4 \text{ mN/rd}$
 $K3 = 3,7 \cdot 10^4 \text{ mN/rd}$
Oldham joint play : $4,36 \cdot 10^{-5} \text{ rd}$
reducer ratio : 100

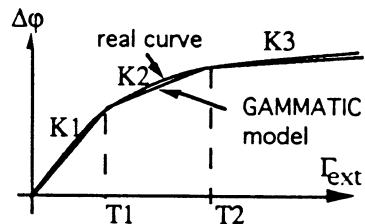


Figure 16



4.2. Mechanic modelization

4.2.1. Parameters of the model

There exist three principal parameters in this reducer which influence the kinematic of the output shaft :

- friction : - between the gear teethes
- on the input bearing shaft
- on the output bearing shaft
- stiffness : - teethes and flexspline displacement
- input shaft and coupling joint
- play : - in the coupling joint
- in the reducer gear

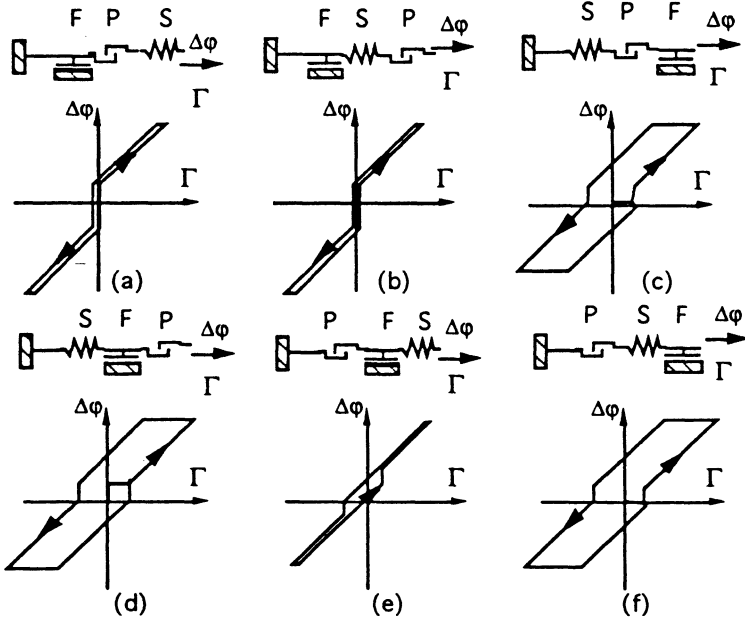


We symbolise each parameter as described on figure 17.

Figure 17 : friction, stiffness and play parameters

4.2.2. Different models

Classically, it is possible to propose different sequential or parallel arrangements of play (P), stiffness (S) and friction (F) parameters. One can see on figure 18 the six serial possibilities. We have tested other combination of serial and parallel arrangements. We propose to choose a model which is adapted to the experimental results.



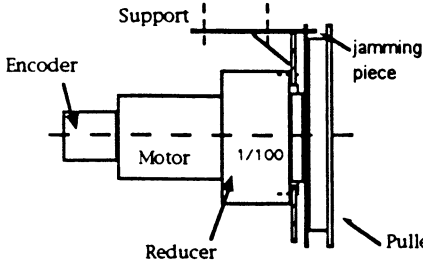
P : play, S : stiffness, F : friction, Γ : applied torque, $\Delta\phi$, angular shift

Figure 18

4.3. Experimentation

4.3.1. Presentation

For measuring the stiffness parameter, we fix the output shaft and apply an electric torque (Γ) as in Charier-Riwan⁵, Seyfferth & coll.¹⁹ (figure 19).



We control the motor with a time varying voltage consign (U_c) (figure 20). We measure the rotation of the input shaft. The preparing cycle is performed in order to regularize the initial conditions of the measurement. The voltage consign is proportional to the electric torque Γ (see § 3.3, equation (7)).

Figure 19 : Scheme of the output shaft jamming

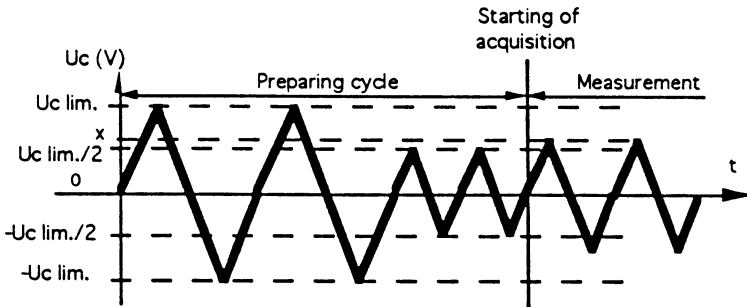


Figure 20 : Graph of the electrical consign U_c

We simultaneously memorize both electrical torque Γ and the angular position of the input shaft. This angular position is multiplied by the transmission ratio (1/100) to report the value on the output shaft.

4.3.2. Results

We present the stiffness characteristics of the RKS 20 - HDUC IH actuator. One can see on figure 21, the measurement of Γ with respect to the angular deformation reported on the output shaft reducer (i.e. multiplied by the ratio). We have drawn the theoretical which is deduced from the Gammatic model (figure 16). We observe that the measured stiffness is lower than this of Gammatic model. The reason is that the reducer output shaft is blocked in our experiment when it is the input shaft in the Gammatic experiment. As it is shown in Gammatic¹¹, the reducer mechanism is not symmetrical with respect to friction and stiffness aspects. So it is natural to obtain a lower stiffness than Gammatic one.

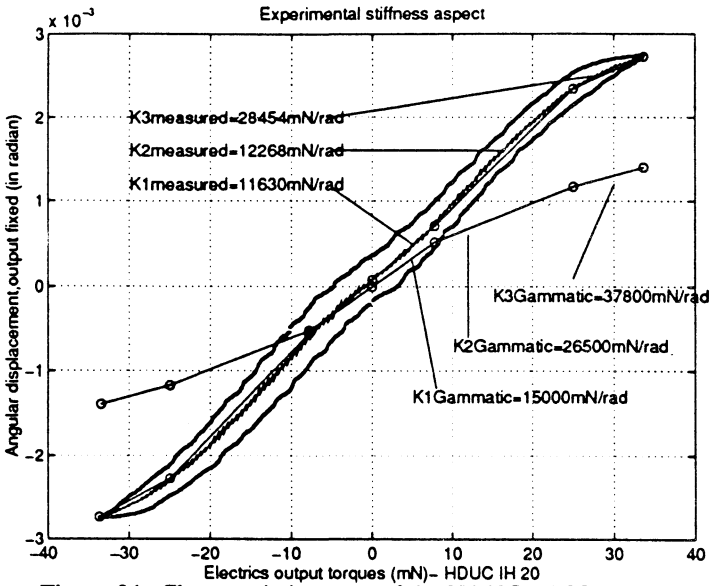


Figure 21- Characteristic curve of the HDUC IH 20 reducer

Figure 22 represents the tangent stiffness value as a function of the electrical torque. This function depends on the numerical filtering.

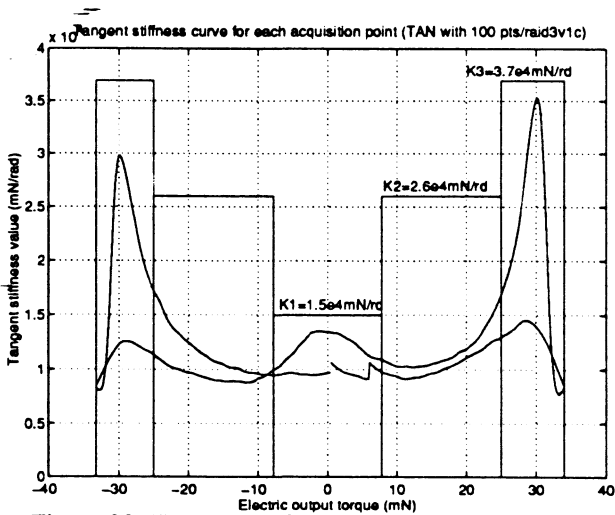


Figure 22- Tangent stiffness of the RKS 20 reducer.

We verify that the hysteresis phenomenon is due to the friction in the reducer. The friction torque corresponds to the semi-bandwidth of the hysteresis curve. Its value depends principally on the maximal applied torque during a cycle (Figure 23).

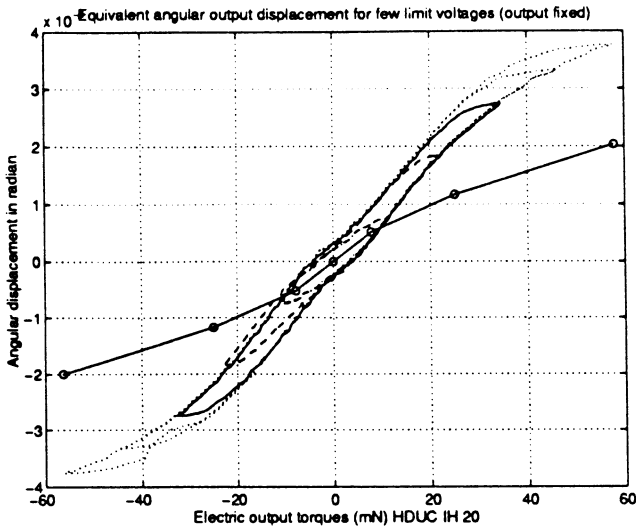


Figure 23 : Stiffness curves with different maximal applied torques

The play parameter does not clearly appear on the curves ; its value is too small with respect to the deformations. We don't observe any starting torque Γ_f s along the experiment.

4.4. Final model

We propose to modelize the transmission with the stiffness-friction-play system (a) of paragraph 4.2.2 (Figure 18c, 18d, 18f) where the play is almost equal to 0, and the stiffness is non linear. Finally, we deduce from this model and the experimental results of figure 21

- stiffness parameters $K_1=1.16 \cdot 10^4$ mN/rd, $K_2=1.23 \cdot 10^4$ mN/rd, $K_3=2.84 \cdot 10^4$ mN/rd,
- play $\neq 0$ rd
- friction torque $\Gamma_f = 2.6$ mN (Γ_f is identified as an equilibrium friction torque Γ_{fe}).

5. CONCLUSION

This paper has described the friction effect in an Harmonic Drive reducer and its stiffness.

We have shown that the variations of the friction torques must be integrated to control laws, because of their importance.

The friction torque depends on angular position. The influence of angular position is slight along a turn of the output shaft (3%). However, there exist two significant hard points per input turn in our Harmonic drive reducer.

The friction torque depends on the external load as described on figure 24.

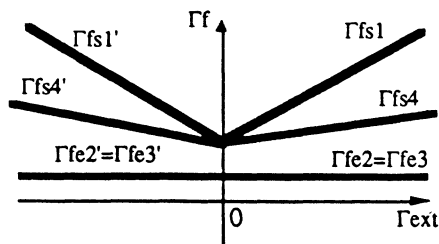


Figure 24 - Friction torque aspect with respect to the pay load.

The symmetry of the Stribeck's model (with respect to the sense of rotation) is not verified for this actuator as soon as there is an external torque Γ_{ext} : $\Gamma_{fs1} \neq \Gamma_{fs4}$. The friction torques are symmetric functions of the external load. The equilibrium friction torque is almost constant. The starting friction torques variations (with the external load) are very important : more than 300% of variation.

The second contribution of this paper concerns the characterization of the stiffness. The measured stiffness coefficients are not equal to those of Gammatic. This is probably due to the difference in the experimental procedure : we fix the output shaft when Gammatic fixes the input shaft. The nonlinearity of the Gammatic model appears in our experiments.

The presented results have been obtained with a Gammatic RKS 20 HDUC IH reducer. The phenomena that we have described there above are confirmed with another reducer (RKS 32 HDUC IH).

Our model is more complete than the usual one and the experimental procedure is general ; we propose to use it in robot identification with either flexible or rigid structures.

The next development concerns the determination of the other parameters of the experimental device of our flexible robot : the inertia of the links and their flexibility.

REFERENCES

- [1] Armstrong B., 1991, "Control of machines with frictions", Kluwer Academic Publishers USA
- [2] Armstrong B., 1993, "Friction modelling methods", a LAN friction Seminar - Ecole centrale de Nantes (LAN)
- [3] Brière, Sabot, Bouchareb, 1988, "Influence des frottements sur la commande dynamique d'un axe de robot" - 7ème Congrès français de la mécanique de Bordeaux.
- [4] Brière, 1991, "Contribution à l'étude du comportement dynamique des réducteurs harmoniques" - Thèse de doctorat 3ème cycle.- Ecole centrale de Lyon (LTS)
- [5] Charier T. Riwan A.- "Caractérisation du réducteur HFUC17_100_2UH sur banc d'essais." Rapport de stage (80 p) C.E.A. CEREM Service de téléopération et de robotique. 92 265 Fontenay-aux-roses .



- [6] Chedmail P., Martineau J.P., 1994, "Validation du modèle de déformation ".- Rapport interne.n°H.94.2 - École centrale de Nantes (LAN) / Ecole navale
- [7] Chedmail P., Martineau J.P., 1995, "Caractérisation des paramètres de frottement d'un réducteur de type Harmonic Drive ".- : Rapport interne.n°H.95.1 - École centrale de Nantes (LAN) / Ecole navale
- [8] Chedmail P., Martineau J.P., 1995, "Modélisation du frottement dans les actionneurs de robots ". AUM - 12è Congrès français de mécanique.
- [9] Depincé P., Chedmail P., Bennis F., "Minimum parameters of flexible links robots - application to a one flexible link" Proc.C. ICAR 1993 Tokyo.
- [10] Gammatic Sarl 11, BUROSPACE - 91572 BIEVRES Cedex - Tél. : (1) 60-19-11-19
- [11] Gammatic : "Torsionnal stiffness of HD Component sets" How to measure the stiffness of an HD reducer , Internal report - 13 p.- GAMMATIC Sarl 11, BUROSPACE 91572 BIEVRES
- [12] Gaudin P., Bessonnet G., "From identification to motion optimisation of a planar manipulator". Robotica 1995 Vol 13 pp 123-132.
- [13] Giovani, Legani, Flagia, 1992 "Harmonic drive transmission : The effect of their elasticity, clearance and irregularity on the dynamic behaviour of an actual Scara robot" - Robotica 92 Vol 10 pp 369-375
- [14] Gogoussis A., Donath M., "Coulomb friction effects on the dynamics of bearings and transmissions in precision robot mechanisms".- IEEE 1988 pp1440-1446.
- [15] Gomes S.C.P., Chrétien J.P., "Dynamic modelling and friction compensated control of a robot manipulator joint".- IEEE ICRA May 1992 Nice France pp 1429-1435.
- [16] Chedmail P., Gautier M.,Pham C.M., "Determination of base parameters of flexible links manipulators".IMAC - Symposium on Modelling and Controle of technological systems, Lille 1991 pp524-529.
- [17] Raymond D., Troncy A., Play D., 1989, "Dynamic characteristics of a manipulator joints".- ASME 1989, VOL 1, pp 447-451.
- [18] Scientific Software 72-78 Grande rue - 92310 SEVRES - Tél. : (1) 45-34-23-91
- [19] Seyffferth W., Maghzal A.J., Angeles J. "Nonlinear modeling and parameter identification of Harmonic Drive robotic transmissions". IEEE ICRA 1995 VOL 3 pp 3027-3032.
- [20] Tuttle T.D., Seering W.P. "Kinematic error, copliance, and friction in a Harmonic Drive gear transmission" ASME Vol 65-1 pp 319-324.